

η mesons in hot and dense asymmetric nuclear matterRajesh Kumar^{*} and Arvind Kumar[†]*Department of Physics, Dr. B. R. Ambedkar National Institute of Technology Jalandhar, Jalandhar 144011, Punjab, India*

(Received 28 November 2020; accepted 10 December 2020; published 29 December 2020)

We study the ηN interactions in the hot and dense isospin asymmetric nuclear matter using two different approaches. In the first approach, the in-medium mass and optical potential of η meson have been calculated in the chiral SU(3) model, considering the effect of explicit symmetry-breaking term and range terms in the ηN interaction Lagrangian density. In the second scenario, the conjunction of chiral perturbation theory and chiral SU(3) model is employed. In this case, the next to leading order ηN interactions are evaluated from the chiral perturbation theory (ChPT), and the in-medium contribution of scalar densities are taken as input from chiral SU(3) model. We observe a larger negative mass shift in the ChPT + chiral model approach compared to the chiral SU(3) model alone as a function of nuclear density. Moreover, the increase in the asymmetry and temperature cause a decrease in the magnitude of mass shift. We have also studied the impact of ηN scattering length $a^{\eta N}$ on the η -meson mass m_η^* and observed that the m_η^* decrease mores for increasing values of scattering length.

DOI: [10.1103/PhysRevC.102.065207](https://doi.org/10.1103/PhysRevC.102.065207)**I. INTRODUCTION**

Meson-baryon interactions are a very important topic of research to study the physics of the nonperturbative QCD regime [1–12]. The heavy-ion collisions (HICs) are used to study the strong-interaction physics by colliding high-energy particles. As a by-product of the collision, the quark gluon plasma (QGP) appears under the utmost conditions of density and temperature [12]. Afterward, with the expansion of a fireball, the QGP cools down and changes its phase to hadronic matter through the hadronization process [12]. These two regimes, i.e., QGP phase and hadronic phase, have different characterization of the respective medium. For example, in the former phase, quarks and gluons act as a degree of freedom, whereas in the latter, mesons and baryons play this role. In the QGP phase the chiral symmetry is followed ($m_q \approx 0$), but in the hadronic phase it is broken explicitly ($m_q \neq 0$) and spontaneously ($\langle \bar{q}q \rangle \neq 0$) [12,13]. Furthermore, in the hadronic ensemble, the thermodynamics quantities namely nuclear density (number density of nucleons), isospin asymmetry (number of neutrons versus the number of protons), and temperature also play crucial roles to modify the in-medium properties of the mesons and baryons [1,2,12].

The operation of future experimental facilities such as compressed baryonic matter (CBM) and antiproton annihilation at Darmstadt (PANDA) at GSI, Germany, nuclotron-based ion collider facility (NICA) at Dubna, Russia and, Japan proton accelerator research complex (J-PARC) at Japan may lead to considerable progress in the understanding of meson-baryons interactions [12,13].

On the theoretical side, several potential models have been theorized to study the physics of the nonperturbative regime.

Some of these are the Nambu-Jona-Lasinio (NJL) model [14], Polyakov loop extended NJL (PNJL) model [15–17], chiral perturbation theory (ChPT) [5,10], coupled channel approach [1,6–8,18], chiral SU(3) model [2,19–28], quark-meson coupling (QMC) model [29–34], Polyakov quark meson (PQM) model [35,36], and QCD sum rules [3,37–41]. Various effective models are formulated, keeping in view the fundamental QCD properties such as broken scale invariance and spontaneous and explicit breaking of the chiral symmetry.

Haider and Liu anticipated that the ηN interactions are attractive and suggested the possibility of η -meson bound states [42,43]. The negative mass-shift and optical potential of the η meson have attracted researchers to study the possibilities of η -mesic nuclei formation [5,10,11]. At nuclear saturation density, the optical potential of -20 MeV was anticipated in the chiral coupled channel approach, considering leading-order terms [11]. Using the same coupled-channel model, Chiang *et al.* obtained optical potential $U_\eta = -34$ MeV in the normal nuclear matter, assuming the ηN interactions dominated by $N^*(1535)$ excitation [44] and anticipated that the attractive potential can produce an η -meson bound state with light and heavy nuclei. Using the QMC model, authors of Ref. [45] obtained the optical potential -60 MeV at $\rho_N = \rho_0$. The chiral unitary approach was also implied to evaluate the η potential and it was observed to be -54 MeV [46]. A more deep optical potential of -72 MeV was observed in Ref. [47]. In this article, the possibility of a bound state with η -meson is also explored.

In Ref. [10], using ηN Lagrangian off-shell terms, at normal nuclear density, the in-medium mass of an η meson was found to be $(0.84 \pm 0.015)m_\eta$ and the corresponding optical potential was observed as $-(83 \pm 5)$ MeV. Furthermore, using the relativistic mean-field theory, Song *et al.* observed the optical potential by varying the scattering length [48]. Clearly, the values of the η optical potential predicted in various studies varies over large range, i.e., -20 to -85 MeV, and

^{*}rajesh.sism@gmail.com[†]kumara@nitj.ac.in

hence have considerable model dependence. In addition to theoretical attempts, there are experimental studies to explore the properties of η mesons [49–54]. For example, for different η -hadron interactions, the η -meson production has been studied in Refs. [49–51] and the transverse momentum spectra of the η meson is measured in HICs near the free N - N production threshold [51].

In the current investigation, we present the in-medium mass and optical potential of the η -meson in hot and dense asymmetric nuclear matter using a chiral SU(3) model. By incorporating the medium-induced nucleon scalar densities, we calculate the in-medium mass shift of the η meson using the ηN effective Lagrangian of the chiral SU(3) model. Furthermore, as discussed earlier, the in-medium mass and optical potential of the η meson have been studied using the unitary approach of ChPT and relativistic mean-field model [10,48]. Following this work, as a second part of the current investigation, the effective mass of the η meson is also evaluated using the chiral ηN Lagrangian of chiral perturbation theory [10]. In this approach, the nucleon scalar densities are calculated from chiral SU(3) model and plugged in the dispersion relation of ηN interactions derived from ChPT Lagrangian.

The chiral SU(3) model is extensively used to explore the in-medium properties of the mesons and baryons in the hot and dense hadronic matter [19,21,55]. For example, the model was used to study the in-medium mass and optical potential of kaons, antikaons, and ϕ mesons in nuclear and hyperonic matter [19,22,26]. Furthermore, in nuclear and hadronic matter, the in-medium mass of spin-0, spin-1 D mesons and quarkonia were calculated using the conjunction of chiral SU(3) model and QCD sum rules with [23–25,56] and without taking the effect of magnetic field [21,57–60]. The model was extended to the SU(4) and SU(5) sectors to evaluate the medium-induced properties of heavy mesons such as D and B [22,27,28]. On the other hand, the chiral perturbation theory is also a successful theoretical framework to study the baryon-meson interactions. The in-medium properties of K meson were first studied by Kaplan and Nelson using chiral perturbation theory (ChPT) [4]. The same theory was applied to study the η -nucleon interactions via adding leading-order terms in the model Lagrangian [5]. The heavy baryon chiral perturbation theory was also applied to study the kaon condensation, which is an imperative property to study the neutron star matter [61–63]. The ChPT theory was also improved by the introduction of next to leading order terms in the chiral effective Lagrangian. By including these off-shell terms, Zhong *et al.* anticipated appreciable decrease in the in-medium mass of the η meson which is favorable for the formation of η -mesic nuclei [10].

The layout of the present paper is as follows: In the next section, we will give a brief explanation of the formalism used in the present work. In Sec. II A 1, we will derive the ηN interactions in the chiral SU(3) model, whereas in Sec. II A 2, ηN methodology will be given in the unified approach of chiral perturbation theory and chiral model. In Sec. III, we will discuss the in-medium effects on the mass of the η meson, and finally in Sec. IV, we will present the summary.

II. FORMALISM

A. In-medium scalar fields in the chiral SU(3) model

The Lagrangian density of the chiral SU(3) model is written as

$$\mathcal{L}_{\text{chiral}} = \mathcal{L}_{\text{kin}} + \sum_{M=S,V} \mathcal{L}_{NM} + \mathcal{L}_{\text{vec}} + \mathcal{L}_0 + \mathcal{L}_{SB}. \quad (1)$$

The model preserves the fundamental QCD properties such as the broken scale invariance and nonlinear realization of the chiral symmetry [2,23,24,64–67]. It is successfully used to explain the nuclear matter, finite nuclei, neutron star, and hypernuclei [2,23,24,64–67]. In this model, the nucleons and baryons interact by the exchange of the vector fields ω and ρ along with the scalar fields σ , ζ , and δ in the nuclear medium. The vector fields give short-range repulsion or attraction which depends on the type of meson-nucleon interaction whereas the scalar fields give attractive contributions to the medium [26]. The σ field is a nonstrange scalar-isoscalar field which represents the scalar mesons σ ($u\bar{d}$), whereas the ζ field is a strange scalar-isoscalar field which represents the scalar meson ($s\bar{s}$) [68]. Moreover, the scalar-isovector field $\delta \approx (\bar{u}u - \bar{d}d)$ is incorporated in the present model to study the effect of the isospin asymmetric matter. Further, the glueball field, χ , is a hypothetical gluon field that contains gluon particles and is introduced in the chiral models to incorporate the scale invariance property of QCD [2,69]. We have used mean-field approximation to simplify the model by neglecting the effect of quantum and thermal fluctuations near phase transitions [23,70].

In Eq. (1), the \mathcal{L}_{kin} term describes the the kinetic energy term and the second term \mathcal{L}_{NM} is given by

$$\mathcal{L}_{NM} = - \sum_i \bar{\psi}_i [m_i^* + g_{\omega i} \gamma_0 \omega + g_{\rho i} \gamma_0 \rho] \psi_i, \quad (2)$$

which defines the nucleon-meson interactions with in-medium nucleon mass as

$$m_i^* = -(g_{\sigma i} \sigma + g_{\zeta i} \zeta + g_{\delta i} \tau_3 \delta), \quad (3)$$

where τ_3 denotes the third component of isospin and $g_{\sigma i}$, $g_{\zeta i}$, and $g_{\delta i}$ are the coupling constants of σ , ζ , and field δ with nucleons ($i = p, n$), respectively. The next term \mathcal{L}_{vec} is given by

$$\mathcal{L}_{\text{vec}} = \frac{1}{2} (m_\omega^2 \omega^2 + m_\rho^2 \rho^2) \frac{\chi^2}{\chi_0^2} + g_4 (\omega^4 + 6\omega^2 \rho^2 + \rho^4), \quad (4)$$

which reproduces the mass of vector mesons through self-interactions. The \mathcal{L}_0 defines the spontaneous chiral symmetry breaking by the equation

$$\begin{aligned} \mathcal{L}_0 = & -\frac{1}{2} k_0 \chi^2 (\sigma^2 + \zeta^2 + \delta^2) + k_1 (\sigma^2 + \zeta^2 + \delta^2)^2 \\ & + k_2 \left(\frac{\sigma^4}{2} + \frac{\delta^4}{2} + 3\sigma^2 \delta^2 + \zeta^4 \right) + k_3 \chi (\sigma^2 - \delta^2) \zeta - k_4 \chi^4 \\ & - \frac{1}{4} \chi^4 \ln \frac{\chi^4}{\chi_0^4} + \frac{d}{3} \chi^4 \ln \left(\left(\frac{(\sigma^2 - \delta^2) \zeta}{\sigma_0^2 \zeta_0} \right) \left(\frac{\chi}{\chi_0} \right)^3 \right). \end{aligned} \quad (5)$$

TABLE I. Different constants used in the present work [2].

Parameter	Value	Parameter	Value	Parameter	Value
k_0	2.53	σ_0 (MeV)	-93.29	$g_{\sigma N}$	10.56
k_1	1.35	ζ_0 (MeV)	-106.8	$g_{\zeta N}$	-0.46
k_2	-4.77	χ_0 (MeV)	409.8	$g_{\delta N}$	2.48
k_3	-2.77	d	0.064	$g_{\omega N}$	13.35
k_4	-0.218	g_4	79.91	$g_{\rho N}$	5.48
m_π (MeV)	139	m_K (MeV)	498	f_π (MeV)	93.29
f_K (MeV)	122.14	ρ_0 (fm ⁻³)	0.15	m_σ (MeV)	466.5
m_ζ (MeV)	1024.5	m_δ (MeV)	899.5	m_η (MeV)	574.374
M_N (MeV)	939				

In this equation, σ_0 , ζ_0 , δ_0 , and χ_0 denote the vacuum values of σ , ζ , δ , and χ scalar fields, respectively. Also, the parameter $d = 0.064$ along with k_i ($i = 1$ to 4) and other

medium parameters are fitted to regenerate the vacuum values of scalar and vector fields, η , η' mesons, and the nucleon mass [2,21,24]. In Table I, we have tabulated the values of various parameters. Furthermore, the last term \mathcal{L}_{SB} in Eq. (1) describes the explicit chiral symmetry breaking property and is written as

$$\mathcal{L}_{SB} = -\left(\frac{\chi}{\chi_0}\right)^2 \left[m_\pi^2 f_\pi \sigma + \left(\sqrt{2} m_K^2 f_K - \frac{1}{\sqrt{2}} m_\pi^2 f_\pi \right) \zeta \right]. \quad (6)$$

In the above equation, m_π , m_K , f_π , and f_K symbolize the masses and decay constants of pions and kaons, respectively.

The nonlinear coupled equations of motion of the scalar and vector fields are deduced by solving the total Lagrangian [Eq. (1)] using the Euler-Lagrange equations [24,25] and are given as

$$k_0 \chi^2 \sigma - 4k_1 (\sigma^2 + \zeta^2 + \delta^2) \sigma - 2k_2 (\sigma^3 + 3\sigma \delta^2) - 2k_3 \chi \sigma \zeta - \frac{d}{3} \chi^4 \left(\frac{2\sigma}{\sigma^2 - \delta^2} \right) + \left(\frac{\chi}{\chi_0} \right)^2 m_\pi^2 f_\pi = \sum g_{\sigma i} \rho_i^s, \quad (7)$$

$$k_0 \chi^2 \zeta - 4k_1 (\sigma^2 + \zeta^2 + \delta^2) \zeta - 4k_2 \zeta^3 - k_3 \chi (\sigma^2 - \delta^2) - \frac{d}{3} \frac{\chi^4}{\zeta} + \left(\frac{\chi}{\chi_0} \right)^2 \left[\sqrt{2} m_K^2 f_K - \frac{1}{\sqrt{2}} m_\pi^2 f_\pi \right] = \sum g_{\zeta i} \rho_i^s, \quad (8)$$

$$k_0 \chi^2 \delta - 4k_1 (\sigma^2 + \zeta^2 + \delta^2) \delta - 2k_2 (\delta^3 + 3\sigma^2 \delta) + 2k_3 \chi \delta \zeta + \frac{2}{3} d \chi^4 \left(\frac{\delta}{\sigma^2 - \delta^2} \right) = \sum g_{\delta i} \tau_3 \rho_i^s, \quad (9)$$

$$\left(\frac{\chi}{\chi_0} \right)^2 m_\omega^2 \omega + g_4 (4\omega^3 + 12\rho^2 \omega) = \sum g_{\omega i} \rho_i^v, \quad (10)$$

$$\left(\frac{\chi}{\chi_0} \right)^2 m_\rho^2 \rho + g_4 (4\rho^3 + 12\omega^2 \rho) = \sum g_{\rho i} \tau_3 \rho_i^v, \quad (11)$$

and

$$k_0 \chi (\sigma^2 + \zeta^2 + \delta^2) - k_3 (\sigma^2 - \delta^2) \zeta + \chi^3 \left[1 + \ln \left(\frac{\chi^4}{\chi_0^4} \right) \right] + (4k_4 - d) \chi^3 - \frac{4}{3} d \chi^3 \ln \left(\left(\frac{(\sigma^2 - \delta^2) \zeta}{\sigma_0^2 \zeta_0} \right) \left(\frac{\chi}{\chi_0} \right)^3 \right) + \frac{2\chi}{\chi_0^2} \left[m_\pi^2 f_\pi \sigma + \left(\sqrt{2} m_K^2 f_K - \frac{1}{\sqrt{2}} m_\pi^2 f_\pi \right) \zeta \right] - \frac{\chi}{\chi_0^2} (m_\omega^2 \omega^2 + m_\rho^2 \rho^2) = 0, \quad (12)$$

respectively.

In the above equations, the ρ_i^s and ρ_i^v denote the scalar and vector densities of i th nucleons ($i = n, p$) [2,24] and are given as

$$\rho_i^v = \gamma_i \int \frac{d^3 k}{(2\pi)^3} \left(\frac{1}{1 + \exp[\beta(E_i^*(k) - \mu_i^*)]} - \frac{1}{1 + \exp[\beta(E_i^*(k) + \mu_i^*)]} \right) \quad (13)$$

and

$$\rho_i^s = \gamma_i \int \frac{d^3 k}{(2\pi)^3} \frac{m_i^*}{E_i^*(k)} \left(\frac{1}{1 + \exp[\beta(E_i^*(k) - \mu_i^*)]} + \frac{1}{1 + \exp[\beta(E_i^*(k) + \mu_i^*)]} \right), \quad (14)$$

respectively, where $\beta = \frac{1}{kT}$, $E_i^*(k) = \sqrt{k^2 + m_i^{*2}}$, $\mu_i^* = \mu_i - g_{\omega i} \omega - g_{\rho i} \tau_3 \rho$, and γ_i is the degeneracy factor. Moreover, the isospin effect on the scalar and vector density is measured by the definition, $I = -\frac{\sum_i \tau_{3i} \rho_i^v}{2\rho_N}$. In the next section, we calculate the medium-modified mass of η mesons in hot asymmetric nuclear matter. The medium modified η -meson mass is evaluated from the dispersion relation which is obtained from the ηN equation of motion.

1. ηN interactions in the chiral $SU(3)$ model

In the chiral $SU(3)$ model, the ηN interaction Lagrangian density can be written as

$$\mathcal{L}_\eta = \left[\frac{1}{2} - \frac{\sigma' + 4\zeta'(2f_K - f_\pi)}{\sqrt{2}f^2} \right] \partial^\mu \eta \partial_\mu \eta - \frac{1}{2} \left[m_\eta^2 - \frac{(\sqrt{2}\sigma' - 4\zeta')m_\pi^2 f_\pi + 8\zeta' m_K^2 f_K}{\sqrt{2}f^2} \right] \eta^2 + \frac{d'}{f^2} \left(\frac{\rho_p^s + \rho_n^s}{4} \right) \partial^\mu \eta \partial_\mu \eta, \quad (15)$$

The above chiral ηN Lagrangian consists of three terms:

- (1) First range term: The first term in the chiral Lagrangian describes the first-range term [2,22] and is obtained from

$$\mathcal{L}_{1\text{strangeterm}} = \text{Tr}(u_\mu X u^\mu X + X u_\mu u^\mu X). \quad (16)$$

In the above equation, $u_\mu = -\frac{i}{2}[u^\dagger(\partial_\mu u) - u(\partial_\mu u^\dagger)]$ and $u = \exp[\frac{i}{\sqrt{2}\sigma_0} P \gamma_5]$, which is expanded up to second order. Here, symbols X and P represent the scalar and pseudoscalar meson matrices [2], respectively, and are explicitly given by Eqs. (A1) and (A2) in the Appendix. Furthermore, the vacuum values of σ and ζ fields are deduced in terms of pions and kaons decay constant by solving the axial current of pions and kaons [2] through the relation

$$\sigma_0 = -f_\pi \quad \zeta_0 = -\frac{1}{\sqrt{2}}(2f_K - f_\pi). \quad (17)$$

Moreover, in the first term of ηN Lagrangian $\sigma' (= \sigma - \sigma_0)$, $\zeta' (= \zeta - \zeta_0)$ and $\delta' (= \delta - \delta_0)$ define the digression of the expectation values of fields from their vacuum expectations. Also, $f = \sqrt{f_\pi^2 + 2(2f_K - f_\pi)^2}$ and $d' = 3d_1 + d_2$ are the constant parameters.

- (2) Mass term: Further, the mass term of the chiral model gives the second term of ηN Lagrangian and is given by

$$\mathcal{L}_{SB} = -\frac{1}{2} \text{Tr} A_p (u X u + u^\dagger X u^\dagger), \quad (18)$$

where A_p is a diagonal matrix given in Eq. (A3). The vacuum mass of the η meson, m_η , is extracted from the

above term and is given by the relation

$$m_\eta = \frac{1}{f} \sqrt{\left(3m_\pi^2 f_K m_K^2 + \frac{8f_K^2 m_K^2}{f_\pi^2} - \frac{4f_K m_\pi^2}{f_\pi} \right)}. \quad (19)$$

When we substitute the values of various constants in the above, m_η turns out to be 574.374 MeV, which is within an accuracy of 4.9% of the physical mass, i.e., 547.862 MeV [71]. The vacuum mass of the η meson has model dependency [72] but here in the present work, we are more concerned in the η in-medium mass shift, which is nearly the same for both the masses. In Ref. [72], using Gell-Mann Okubo mass formula under octet approximation in the $SU(4)$ meson multiplets, the authors calculated the vacuum mass of the η meson to be 567 MeV, which is within an accuracy of 3.6%.

- (3) d' term: The third term (i.e., d' term) in the ηN Lagrangian originates from the baryon-meson interaction Lagrangian densities [20,27]

$$\mathcal{L}_{d_1}^{BM} = \frac{d_1}{2} \text{Tr}(u_\mu u^\mu) \text{Tr}(\bar{B}B) \quad (20)$$

and

$$\mathcal{L}_{d_2}^{BM} = d_2 \text{Tr}(\bar{B}u_\mu u^\mu B). \quad (21)$$

In the above, B denotes the baryon matrix [see Eq. (A4)].

It should be noted that in case of ηN interactions of Eq. (15), the terms corresponding to vectorial Weinberg-Tomozawa term vanishes. On the other hand, the Weinberg-Tomozawa term plays a crucial role in the determination of $K(\bar{K})$ and $D(\bar{D})$ in-medium mass [22,28].

Using the ηN Lagrangian in the Euler-Lagrange equation for η meson, the equation of motion is evaluated as

$$\partial^\mu \partial_\mu \eta - \left(m_\eta^2 - \frac{(\sqrt{2}\sigma' - 4\zeta')m_\pi^2 f_\pi + 8\zeta' m_K^2 f_K}{\sqrt{2}f^2} \right) \eta + \frac{2d'}{f^2} \left(\frac{\rho_p^s + \rho_n^s}{4} - \frac{\sigma' + 4\zeta'(2f_K - f_\pi)}{\sqrt{2}} \right) \partial^\mu \partial_\mu \eta = 0. \quad (22)$$

Performing the Fourier transformation on the above equation, the dispersion relation for η meson turns out to be

$$-\omega^2 + \mathbf{k}^2 + m_\eta^2 - \Pi^*(\omega, |\mathbf{k}|) = 0. \quad (23)$$

In the above equation, Π^* denotes the effective self-energy of η meson, explicitly given as

$$\Pi^*(\omega, |\mathbf{k}|) = -\frac{(\sqrt{2}\sigma' - 4\zeta')m_\pi^2 f_\pi + 8\zeta' m_K^2 f_K}{\sqrt{2}f^2} + \frac{2d'}{f^2} \left(\frac{\rho_p^s + \rho_n^s}{4} \right) (\omega^2 - \bar{k}^2) - \frac{2}{f^2} \left[\frac{\sigma' + 4\zeta'(2f_K - f_\pi)}{\sqrt{2}} \right] (\omega^2 - \mathbf{k}^2). \quad (24)$$

The unknown parameter, d' , is approximated from the experimental values of scattering length, $a^{\eta N}$ [10]. In the chiral model, the expression of scattering length derived from the scattering amplitude is given by

$$a^{\eta N} = \frac{1}{4\pi(1 + \frac{m_\eta}{M_N})} \left[\left(\frac{d'}{\sqrt{2}} - \frac{g_{\sigma N}}{m_\sigma^2} + \frac{4(2f_K - f_\pi)g_{\zeta N}}{m_\zeta^2} \right) \frac{m_\eta^2}{\sqrt{2}f^2} + \left(\frac{\sqrt{2}g_{\sigma N}}{m_\sigma^2} - \frac{4g_{\zeta N}}{m_\zeta^2} \right) \frac{m_\pi^2 f_\pi}{2\sqrt{2}f^2} + \tau_3 \frac{2\sqrt{2}g_{\delta N} m_K^2 f_K}{m_\delta^2 f^2} \right]. \quad (25)$$

Rearranging the above for d' gives

$$d' = \frac{f^2}{2\pi(1 + \frac{m_\eta}{M_N})} \frac{a^{\eta N}}{m_\eta^2} + \frac{\sqrt{2}g_{\sigma N}}{m_\sigma^2} - \frac{4\sqrt{2}(2f_K - f_\pi)g_{\zeta N}}{m_\zeta^2} - \left(\frac{\sqrt{2}g_{\sigma N}}{m_\sigma^2} - \frac{4g_{\zeta N}}{m_\zeta^2} \right) \frac{m_\pi^2 f_\pi}{\sqrt{2}m_\eta^2} - \tau_3 \frac{4\sqrt{2}g_{\delta N} m_K^2 f_K}{m_\delta^2 m_\eta^2}. \quad (26)$$

Using the condition, $m_\eta^* = \omega(|\mathbf{k}| = 0)$ in Eq. (23), we obtain the effective mass of η meson in the nuclear medium. Further, the momentum-dependent optical potentials are defined through the relation [28,73]

$$U_\eta^*(\omega, \mathbf{k}) = \omega(\mathbf{k}) - \sqrt{\mathbf{k}^2 + m_\eta^2}. \quad (27)$$

At zero momentum, the above equation gives

$$U_\eta^* = \Delta m_\eta^* = m_\eta^* - m_\eta. \quad (28)$$

2. Unification of chiral perturbation theory (ChPT) and chiral model

In this section, we discuss the unified approach of ChPT and chiral model to compute the in-medium mass of η mesons. The ChPT comprises the underlying chiral symmetry property of QCD and use an effective field theory approach [10]. The same theory along with the relativistic mean-field model has been used to deduce the η -nucleon interactions in the symmetric nuclear matter [10,48]. The Lagrangian density defining the meson-baryons interactions in this theory is given by

$$\mathcal{L}_{\text{ChPT}} = \mathcal{L}_P + \mathcal{L}_{PB}, \quad (29)$$

with P representing the pseudoscalar meson multiplet [see Eq. (A2)]. Up to second chiral order, the \mathcal{L}_P term is defined as [4,10]

$$\mathcal{L}_P = \frac{1}{4} f_\pi^2 \text{Tr} \partial^\mu \Sigma \partial_\mu \Sigma^\dagger + \frac{1}{2} f_\pi^2 B_0 \{ \text{Tr} M_q (\Sigma - 1) + \text{H.c.} \}, \quad (30)$$

where $\Sigma = \xi^2 = \exp(i\sqrt{2}P/f_\pi)$ and $M_q = \text{diag}\{m_q, m_q, m_s\}$ is the current quark mass matrix. The Lagrangian term $\mathcal{L}_{PB} = \mathcal{L}_{PB}^L + \mathcal{L}_{PB}^{NL}$ describes the leading and next to leading order contributions [4]. Jenkins and Manohar developed the next to leading order terms using heavy baryon chiral theory [5]. In this Lagrangian, the loop contributions not considered as higher order corrections get suppressed for the small momentum scale, Q^2 [10]. The different nuclear properties are studied successfully using \mathcal{L}_{PB}^{NL} [74].

The ηN Lagrangian is obtained by expanding Eq. (29) up to the second order of multiplet P [10]

$$\begin{aligned} \mathcal{L}_{\eta N} = & \frac{1}{2} \partial^\mu \eta \partial_\mu \eta - \frac{1}{2} \left(m_\eta^2 - \frac{\Sigma_{\eta N}}{f_\pi^2} \bar{\Psi}_N \Psi_N \right) \eta^2 \\ & + \frac{1}{2} \frac{\kappa}{f_\pi^2} \bar{\Psi}_N \Psi_N \partial^\mu \eta \partial_\mu \eta. \end{aligned} \quad (31)$$

Here, $m'_\eta = \sqrt{\frac{2}{3} B_0 (m_q + 2m_s)}$ denotes the vacuum mass of the η meson calculated in chiral perturbation theory. In the mass expression, B_0 symbolizes the relation with the order parameter of spontaneously broken chiral symmetry and $m_{q(s)}$ denotes the mass of light (strange) quarks [72]. For consistency with the chiral SU(3) model, we have used the same value of η meson vacuum mass, i.e., $m'_\eta = m_\eta = 574.374$ MeV in the further calculations of ChPT. The ηN sigma term $\Sigma_{\eta N}$, obtained from “ a_i ” terms of the next to leading order chiral Lagrangian density, is given as [10]

$$\Sigma_{\eta N} = -\frac{2}{3} [a_1 m_q + 4a_2 m_s + 2a_3 (m_q + 2m_s)]. \quad (32)$$

The $\Sigma_{\eta N}$ value is estimated to be 280 ± 130 MeV from the different empirical observations of Σ_{KN} term having value 380 ± 100 MeV [10,61,62,75–79].

Also, the parameter κ in the last term of Eq. (31) comprises the contributions from the “off-shell” d_i terms of the next to leading order Lagrangian [10]. In the present work, we determined κ using the expression of ηN scattering length, $a^{\eta N}$, calculated from the ChPT matrix amplitude (on-shell constraints) [10]

$$a^{\eta N} = \frac{1}{4\pi f_\pi^2 (1 + m_\eta/M_N)} (\Sigma_{\eta N} + \kappa m_\eta^2), \quad (33)$$

and by rearranging for κ it becomes

$$\kappa = 4\pi f_\pi^2 \left(\frac{1}{m_\eta^2} + \frac{1}{m_\eta M_N} \right) a^{\eta N} - \frac{\Sigma_{\eta N}}{m_\eta^2}. \quad (34)$$

We have taken the experimentally determined $a^{\eta N}$ values, i.e., ≈ 0.91 – 1.14 fm in the present investigation [10,80–83]. Furthermore, the ηN equation of motion has been derived using the interaction Lagrangian [Eq. (31)] in the Euler Lagrange equation of motion:

$$\left(\partial_\mu \partial^\mu + m_\eta^2 - \frac{\Sigma_{\eta N}}{2f_\pi^2} \langle \bar{\Psi}_N \Psi_N \rangle + \frac{\kappa}{2f_\pi^2} \langle \bar{\Psi}_N \Psi_N \rangle \partial_\mu \partial^\mu \right) \eta = 0. \quad (35)$$

In the above, $\langle \bar{\Psi}_N \Psi_N \rangle \equiv \rho_N^s = (\rho_p^s + \rho_n^s)$ defines the in-medium scalar density of nucleons calculated within the mean-field chiral SU(3) model [see Eqs. (13) and (14)]. The Fourier transformation of Eq. (35) gives

$$-\omega^2 + \mathbf{k}^2 + m_\eta^2 - \frac{\Sigma_{\eta N}}{2f_\pi^2} \rho_N^s + \frac{\kappa}{2f_\pi^2} \rho_N^s (-\omega^2 + \mathbf{k}^2) = 0. \quad (36)$$

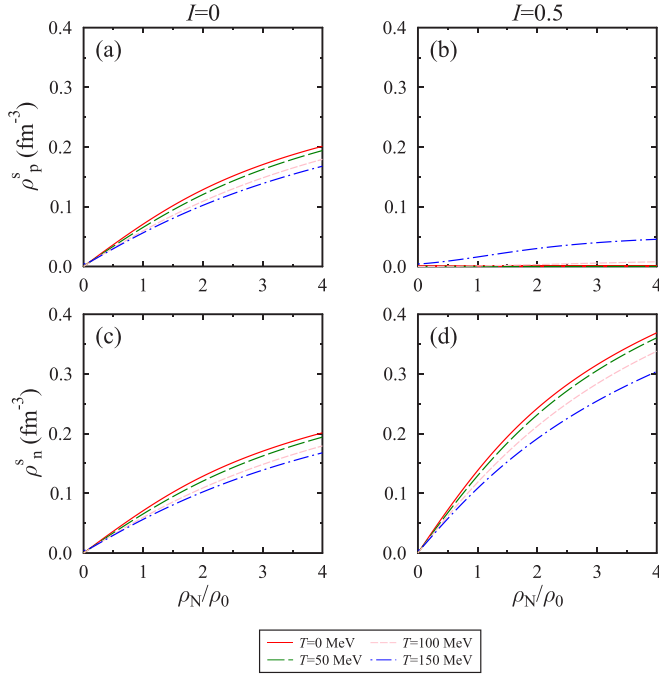


FIG. 1. The in-medium scalar density of nucleons.

From the above equation, the effective mass $m_\eta^* = \omega(|\mathbf{k}|=0)$ of η meson can be written as

$$m_\eta^* = \sqrt{\left(m_\eta^2 - \frac{\Sigma_{\eta N}}{2f_\pi^2} \rho_N^s\right) / \left(1 + \frac{\kappa}{2f_\pi^2} \rho_N^s\right)}. \quad (37)$$

Further, the η -meson self-energy derived from Eq. (36) is given by

$$\Pi^*(\omega, \mathbf{k}) = \left[-\frac{\Sigma_{\eta N}}{2f_\pi^2} + \frac{\kappa}{2f_\pi^2} (-\omega^2 + \mathbf{k}^2) \right] \rho_N^s. \quad (38)$$

III. RESULTS AND DISCUSSION

In this section, first we discuss the behavior of in-medium nucleon scalar densities in the hot asymmetric nuclear matter. Further, we discuss the effective mass of the η meson, which is derived using the chiral SU(3) model alone in Sec. III A and with the unified approach of ChPT and chiral SU(3) model in Sec. III B. In both approaches, we show the results for range of scattering length, $a^{\eta N} = 0.91$ – 1.14 fm. Various parameters used in the present investigation are mentioned in Table I.

In the chiral model, the scalar densities of nucleons have been calculated through Eq. (14). This equation contains the effect of medium modified scalar and vector fields [2]. The in-medium behavior of these fields is obtained by solving the coupled equations of motion [Eqs. (7) to (12)] [26]. In Fig. 1, we plot the scalar density of proton and neutron as a function of number density for finite values of temperature, T , and isospin asymmetry parameter. In symmetric nuclear matter, as the contribution of δ and ρ field is zero [24], we get the same behavior of neutron and proton scalar densities. The δ and ρ fields change the in-medium value of baryon mass m_i^* and effective chemical potential μ_i^* , respectively, which

further modify the nucleon scalar density [see Eq. (14)] [2]. In the figure, at $T = 0$ the scalar density increases linearly in the low-density regime and becomes nonlinear in the high-density regime. When we move from the $I = 0$ to $I \neq 0$ region, we observe a gradual increase in the neutron scalar density, whereas the proton scalar density decreases. This is because of the nonzero contribution of δ and ρ fields in the isospin asymmetric nuclear matter, which changes the effective mass as well as chemical potential and therefore scalar density [2].

Another thermodynamic quantity, i.e., temperature, is also a main property of the nuclear medium, and in Fig. 1 we have shown how the in-medium dynamics changes under nonzero temperature. The effect of temperature is observed more in the high-density regime as compared to the low-density regime. For symmetric matter in Figs. 1(a) and 1(c), we anticipate an appreciable effect of temperature. Here, for a particular value of nuclear density, the value of scalar densities decrease as a function of temperature. Because of the Fermi distribution integral, due to the coupled nature of Eqs. (7) to (12), the value of scalar density in Eq. (14) decreases when we increase the temperature in the integral. On the other hand, in the highly asymmetric matter, i.e., $I = 0.5$, for the neutron scalar density the temperature effects become more appreciable. In addition, we observe a minor contribution to the proton scalar density for higher temperature values. This is because at finite temperature the proton condensate ($\bar{p}p$), i.e., proton scalar density still populates in the medium despite the zero value of proton number density ρ_p . The observed behavior of scalar densities in the symmetric nuclear matter is in agreement with the calculations of the relativistic mean-field model [10,48].

A. Optical potential and mass of η meson in chiral model

In Fig. 2, we have illustrated the medium modified mass of the η meson as a function of nuclear density for different values of scattering length. In the same figure, we also show the impact of isospin asymmetry and temperature. For a given value of asymmetry, temperature, scattering length, the in-medium mass of the η meson is observed to decrease as a function of nuclear density. The rate of decrease is linear in the low-density regime, whereas in the high-density regime it becomes nonlinear. This behavior reflects the opposite variation of nucleon scalar density plotted in Fig. 1. This is because the self-energy of the η meson [see Eq. (24)] has a direct dependence on the sum of scalar densities of nucleons.

When we change the value of $a^{\eta N}$ from 0.91 to 1.14 fm, we observe a decrement in the effective mass. For example, at $\rho_N = \rho_0(4\rho_0)$, $I = T = 0$, the effective mass of η meson changes from 528 (441) to 512 (423) MeV when we change the $a^{\eta N}$ value from 0.91 to 1.14 fm, respectively. This is due to the d' term in Eq. (24). The d' term has direct dependence on $a^{\eta N}$ as shown in Eq. (26) and therefore increases the value of scattering length, causing an increase in the value of d' . Due to the attractive contribution of the self-energy part corresponding to the d' term, the value of effective mass decreases. We also observed the substantial impact of the temperature on the in-medium mass in the symmetric nuclear matter which reflects the in-medium behavior of scalar densities. However, in the asymmetric nuclear matter, we observe

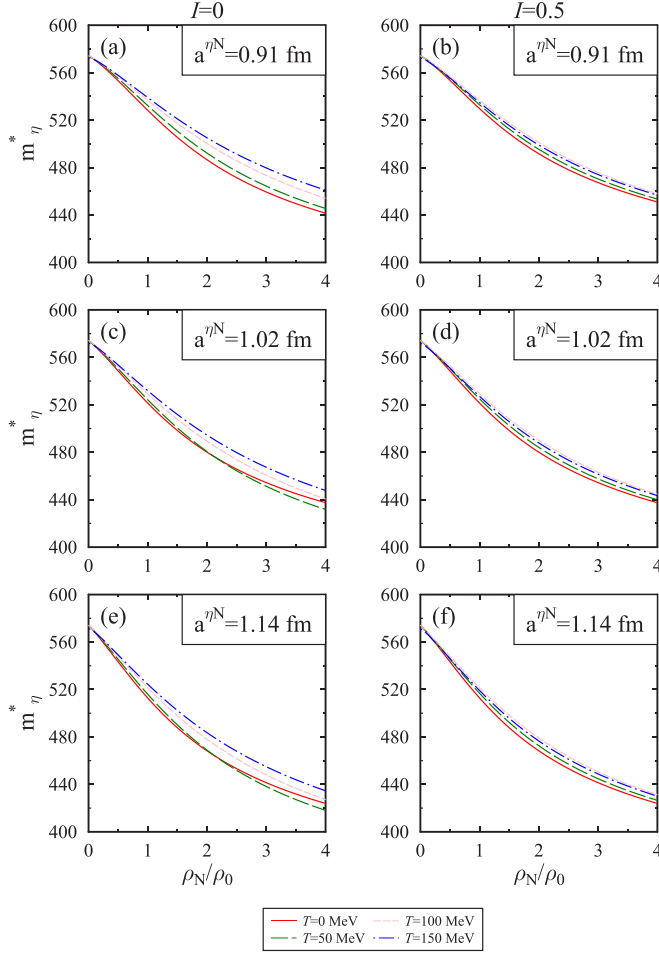


FIG. 2. In-medium η -meson mass in the chiral model.

the temperature effects on the mass to be less appreciable which reflects the less contribution of the net scalar density ($\rho_p^s + \rho_n^s$).

The self-energy expression given by Eq. (24) contains three terms: (i) first range term, (ii) mass term, and (iii) d' term. To understand the contribution of these individual terms, we illustrated the in-medium mass of the η meson at zero and nonzero values of asymmetry and temperature in Fig. 3 for these different terms. At zero temperature and asymmetry, one can see that the first range term gives an appreciable repulsive contribution to the effective mass whereas the mass and d' terms give attractive contributions. We observe the dominant contribution of the d' term, which in turn gets reflected in the net effective mass. For nonzero temperature and asymmetry, the variation in the d' term becomes less and hence we get a lower value of effective mass. This is due to the effect of scalar density terms present in the d' term [Eq. (24)]. For further understanding, in Fig. 4 we plot the η -meson effective mass as a function of scattering length $a^{\eta N}$ at $\rho_N = \rho_0, 4\rho_0$. At nuclear saturation density, we observe a linear decrease of effective mass with the increase in scattering length. Furthermore, the effective mass decrease more rapidly in the high-density regime. The observed behavior emphasizes the importance of scattering length in the ηN interactions.

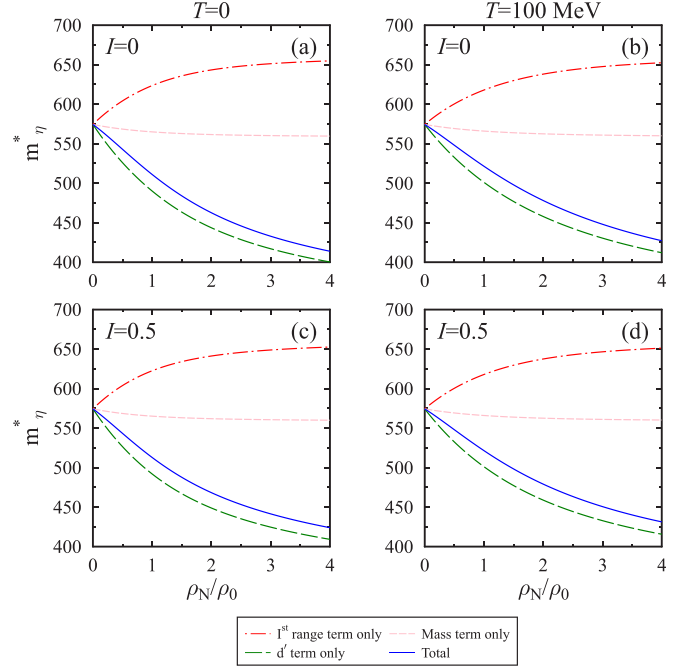


FIG. 3. Comparison of the different terms of η -meson effective mass in chiral model at $a^{\eta N} = 1.14$ fm.

The decrease in the in-medium mass leads to a negative mass shift which suggests the bound-state formation of an η meson with a nucleus [5,10]. To understand the bound-state phenomenon, the study of in-medium optical potential is imperative. By using the effective mass in Eq. (28), we plotted the optical potential of an η meson as a function of

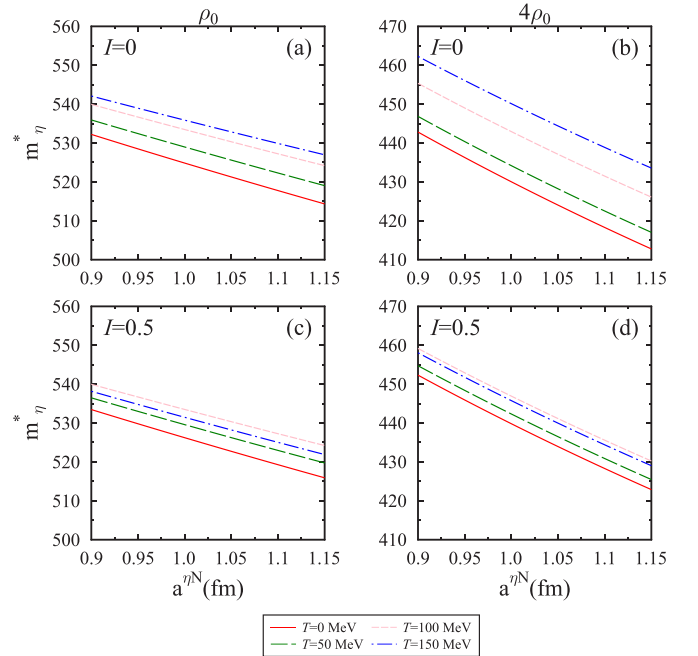


FIG. 4. The in-medium η -meson mass as a function of scattering length.

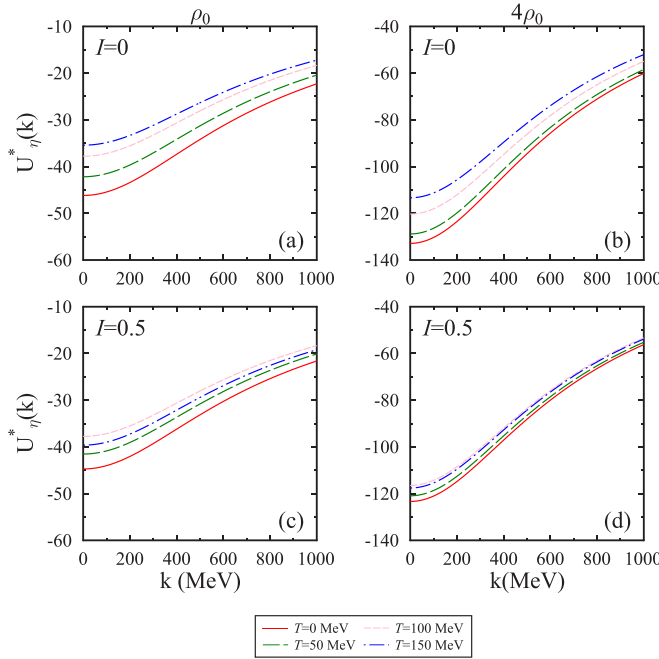


FIG. 5. The in-medium η meson optical potential in chiral model at $a^{\eta N} = 0.91$ fm.

momentum $|\mathbf{k}|$ for different values of ηN scattering length and other medium parameters in Figs. 5–7. In Fig. 5, at $\rho_N = \rho_0$ we observe a negative value of the optical potential. The value of optical potential becomes less negative as we increase the momentum of the η meson. The variation of optical potential reflects the interplay between the effective mass and momentum. At high values of the momentum, Eq. (28) gets

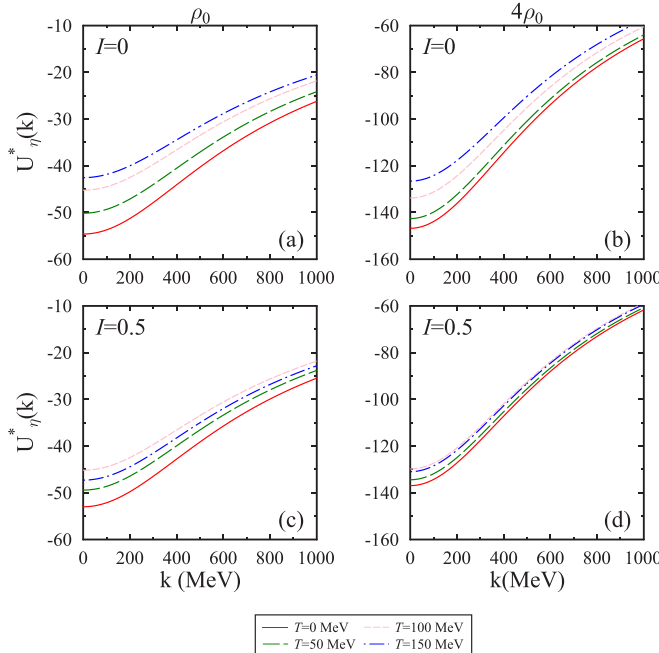


FIG. 6. The in-medium η -meson optical potential in chiral model at $a^{\eta N} = 1.02$ fm.

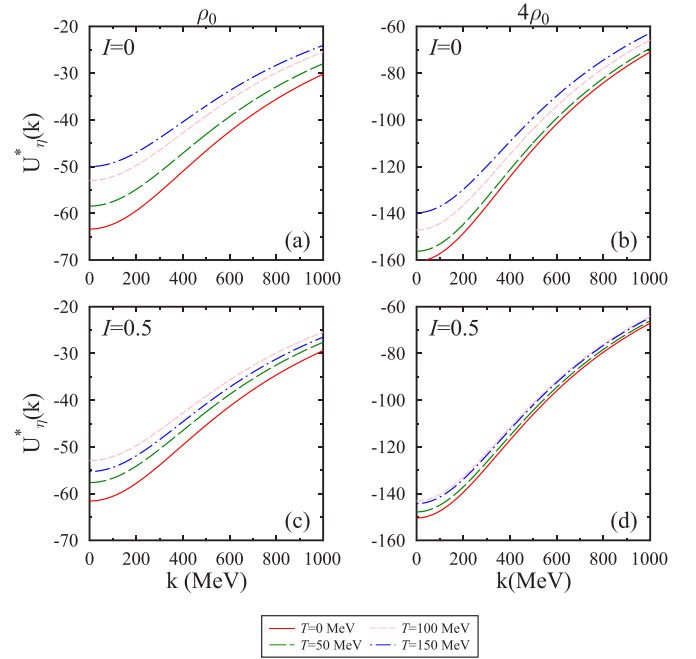


FIG. 7. The in-medium η meson optical potential in chiral model at $a^{\eta N} = 1.14$ fm.

dominated by momentum and the contribution of effective mass becomes less.

A similar phenomenon happens in the high-density regime. In this region, we observe appreciable values of optical potential which become less as momentum increases. Moreover, in the presence of a high density of neutron matter, we anticipate less effect of temperature, which reflects the in-medium behavior of the η -meson mass. In Figs. 6 and 7, we observe a similar trend of optical potential with η momentum. In these figures, we observe a more negative value of optical potential as we increase the scattering length. As discussed earlier, the optical potential is directly related to in-medium mass, and here it is illustrated to get a clear idea of negative potential. In the cold symmetric nuclear matter, at $\rho_N = \rho_0(4\rho_0)$ we observe optical potential to be -54.61 (-146.77) MeV for $a^{\eta N} = 1.02$ fm, whereas for $I = 0.5$ these values change to -52.99 (-136.93) MeV. For better understanding, we have tabulated the in-medium mass shift of the η meson at zero momentum in Table II.

B. In-medium mass of η meson in unified approach of ChPT and chiral model

In this section, we have used the unified approach of the chiral SU(3) model and chiral perturbation theory to calculate the medium-induced mass of the η meson. As discussed in the methodology section, the ηN equation of motion is obtained from the Lagrangian density of ChPT. Further, the scalar density of nucleons appearing in the ChPT equation of motion is obtained from the chiral SU(3) model. In this calculation, we have taken the value of parameter $\Sigma_{\eta N}$ to be 280 MeV. We have not considered the contribution of uncertainties in the $\Sigma_{\eta N}$ parameter because of the lesser contribution of the σ term

TABLE II. Values of in-medium mass-shift of the η meson for different medium attributes calculated in the chiral model (in units of MeV).

a^{nN} (fm)	$\eta = 0$				$\eta = 0.5$				
	$T = 0$		$T = 100$		$T = 0$		$T = 100$		
	ρ_0	$4\rho_0$	ρ_0	$4\rho_0$	ρ_0	$4\rho_0$	ρ_0	$4\rho_0$	
Δm_η^*	0.91	-46.18	-132.88	-37.78	-120.31	-44.74	-123.35	-37.74	-116.46
	1.02	-54.61	-146.77	-45.22	-133.79	-52.99	-136.93	-45.16	-129.78
	1.14	-63.37	-160.51	-52.98	-147.21	-61.58	-150.42	-52.92	-143.07

in the in-medium mass as compared to the κ term, which we will see later. The values of in-medium η mass shift calculated using the present unified approach are given in Table III.

In Fig. 8, we illustrated the ratio of the in-medium and vacuum mass of the η meson as a function of nuclear density. In this figure, we have also included the effect of η/N scattering length, temperature, and medium isospin asymmetry. Moreover, we compared the results obtained from two different approaches, i.e., (i) chiral model alone and (ii) ChPT and chiral model. Using the second approach, we observed a substantial decrease in the mass of the η meson. We observed the same behavior of the in-medium mass with respect to temperature, asymmetry, and scattering length as was observed in the situation when the chiral model was used alone. The main difference is that in the ChPT the η meson gets a more net attractive contribution than the chiral model, which is due to the absence of the first range term in ChPT Lagrangian. In Fig. 9, we have plotted the contributions of individual terms to the in-medium mass of the η meson calculated from the unified approach. The η -meson in-medium mass given by Eq. (37)

in the ChPT + chiral model approach has two terms: the (i) $\Sigma_{\eta N}$ term and (ii) κ term. In this figure, we have shown the individual contribution of these terms with increasing nuclear density and observed a nonappreciable contribution with $\Sigma_{\eta N}$ but appreciable with κ term. This is because in the η -meson in-medium mass expression [see Eq. (37)], the denominator has a positive contribution of the scalar densities and the increase in scalar density with number density increases the denominator hence the value of effective mass becomes more negative. Clearly, there is no first range term with the positive contribution as was observed in the previous chiral model calculations, and therefore in the present case we get substantial attractive mass shift.

The present observations can be compared with the η -meson effective mass calculated in the unified approach of ChPT and relativistic mean-field model of Ref. [10]. In this article, the authors also considered the effect of scattering length and at nuclear saturation density and $a^{nN} = 1.02$ fm they anticipated the effective mass to be $0.84 m_\eta$, whereas we observed it to be $0.79 m_\eta$. At nuclear saturation density,

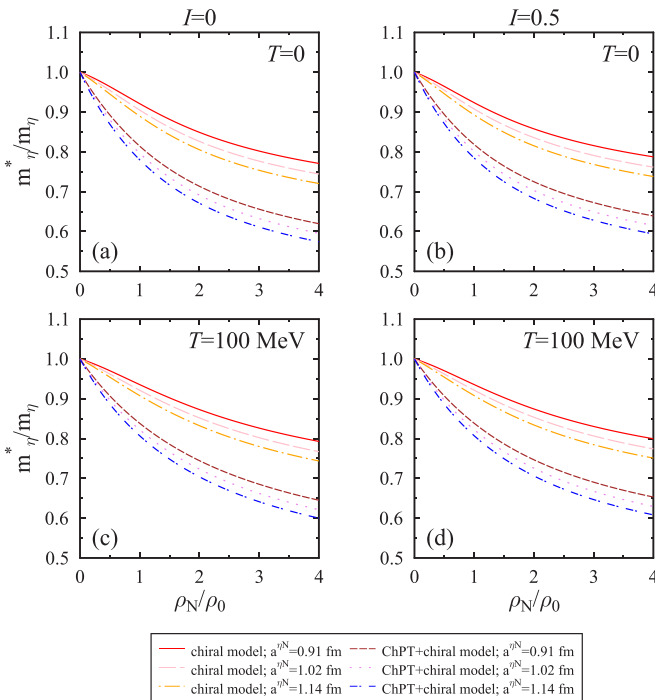


FIG. 8. Comparison of in-medium η -meson mass calculated from chiral model and ChPT.

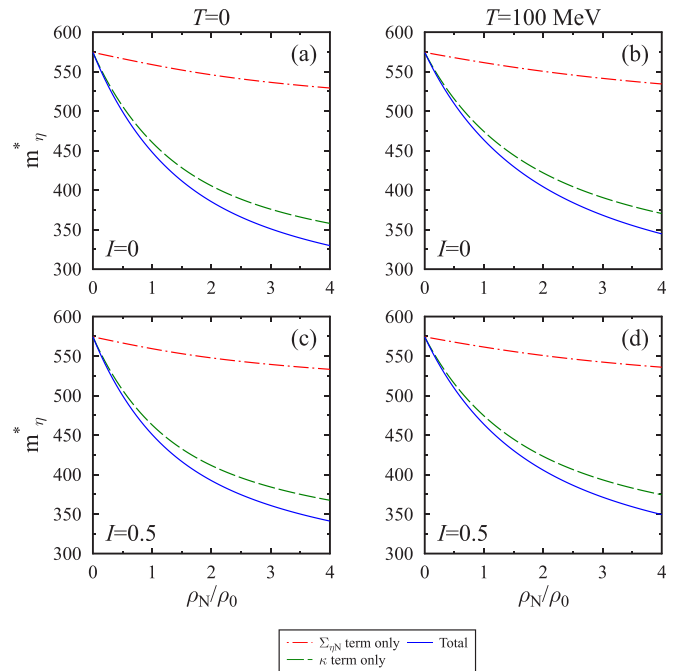


FIG. 9. Comparison of different terms of the effective mass of η meson calculated using unification of ChPT and chiral model at $a^{nN} = 1.14$ fm.

TABLE III. Values of in-medium mass-shift of η -meson for different medium attributes calculated in the ChPT+chiral model are tabulated (in units of MeV).

	a^{nN} (fm)	$\eta = 0$				$\eta = 0.5$			
		$T = 0$		$T = 100$		$T = 0$		$T = 100$	
		ρ_0	$4\rho_0$	ρ_0	$4\rho_0$	ρ_0	$4\rho_0$	ρ_0	$4\rho_0$
Δm_η^*	0.91	-107.54	-219.71	-93.73	-205.06	-105.19	-208.52	-93.64	-200.43
	1.02	-116.83	-232.28	-102.21	-217.49	-114.35	-220.99	-102.11	-212.80
	1.14	-126.36	-244.56	-110.96	-229.72	-123.75	-233.24	-110.86	-225.00

the effective mass equal to $0.95 m_\eta$ was obtained within the coupled channel approach with scattering length $a^{nN} \approx 0.25$ fm [11]. In this nondiagonal coupled channel approach, there are only leading-order contributions and hence only a small decrement in the in-medium mass is observed. Also, in the QMC model at ρ_0 the in-medium mass of the η meson having value $0.88 m_\eta$ was observed [45]. The obtained values are comparable with the calculations of the ChPT+chiral model for $a^{nN} \approx 0.50$ fm.

In the cold symmetric nuclear matter, at $\rho_N = \rho_0(4\rho_0)$ and $|\mathbf{k}| = 0$, we observe optical potential to be -116.83 (-232.28) MeV for $a^{nN} = 1.02$ fm and in the cold isospin asymmetric nuclear matter the values modifies to -114.35 (-220.99) MeV. Using the ChPT + chiral model approach, we observed a even deeper optical potential than evaluated in the relativistic mean-field model + ChPT approach of Ref. [10]. This is due to the difference in the in-medium scalar densities obtained in two models. In our approach, we have taken the effect of scalar and vector fields under the influence of isospin asymmetry and finite temperature whereas in the relativistic model approach only cold symmetric medium was considered. The η optical potential was also observed in the different theoretical observations [9–11,45,46]. $U_\eta = -34$ MeV was observed by studying the ηN interactions near the threshold using the free space chirally inspired coupled-channel approach by considering the contributions of $N^*(1535)$ baryon resonance [9]. Besides, the optical potential $U_\eta = -54, -60,$ and -83 MeV was observed in the chiral unitary approach [46], QMC model [45], and the ChPT [10], respectively.

IV. SUMMARY

We investigated the in-medium mass of the η meson in the asymmetric nuclear matter at finite temperature. Under these

medium conditions, we studied the behavior of the η meson using two different methodologies. In the first methodology, using the chiral model alone, we calculated the medium modified mass and optical potential of the η meson by considering the ηN interactions up to second order in the Lagrangian and observed a decrease in the effective mass of the η meson as a function of density. We find the in-medium effects to be more appreciable in the high-density regime. In the second, we used the unified approach of chiral perturbation theory (ChPT) and chiral SU(3) model to study the in-medium attributes of the η meson. In this approach, we took the next to leading order contributions. We incorporated the medium effects from the chiral SU(3) model through scalar density which is plugged in the ηN equation of motion, which is calculated from the effective ηN Lagrangian of ChPT. Using this methodology, we find a substantial decrease in the mass of the η meson as a function of nuclear density. The temperature and asymmetry effects are also studied and found to be slight repulsive in nature. Also, in the both approaches the mass shift is observed to increase with an increase in the value of scattering length. The decrement on the η -meson mass leads to a negative mass shift and optical potential which further suggests the possibility of ηN bound states. The optical potential calculated in the present work will be used in future to calculate the spectroscopic state of the η -mesic nuclei [10]. Also, the momentum-dependent optical potential can be used to study the η -meson production rate [49–51] and its momentum dependence in the asymmetric nuclear medium [52,84,85].

ACKNOWLEDGMENTS

One of the authors (R.K.) sincerely acknowledges the support of this work from Ministry of Science and Human Resources Development (MHRD), Government of India, via the National Institute of Technology Jalandhar.

APPENDIX: EXPLICIT REPRESENTATION OF DIFFERENT MATRICES

Here, we give the matrix representation of meson, baryon, and mass matrices which are used in the present calculations [2]:

(1) The scalar meson matrix, X :

$$X = \frac{1}{\sqrt{2}} \sigma^a \lambda_a = \begin{pmatrix} (\delta + \sigma)/\sqrt{2} & \delta^+ & \kappa^+ \\ \delta^- & (-\delta + \sigma)/\sqrt{2} & \kappa^0 \\ \kappa^- & \kappa^0 & \zeta \end{pmatrix}. \quad (\text{A1})$$

(2) The pseudoscalar meson matrix, P :

$$P = \frac{1}{\sqrt{2}} \pi_a \lambda^a = \begin{pmatrix} \frac{1}{\sqrt{2}} \left(\pi^0 + \frac{\eta}{\sqrt{1+2w^2}} \right) & \pi^+ & 2 \frac{K^+}{w+1} \\ \pi^- & \frac{1}{\sqrt{2}} \left(-\pi^0 + \frac{\eta}{\sqrt{1+2w^2}} \right) & 2 \frac{K^0}{w+1} \\ 2 \frac{K^-}{w+1} & 2 \frac{\bar{K}^0}{w+1} & -\frac{\eta\sqrt{2}}{\sqrt{1+2w^2}} \end{pmatrix}, \quad (\text{A2})$$

where $w = \sqrt{2}\zeta_0/\sigma_0$.

(3) The A_p matrix:

$$A_p = \frac{1}{\sqrt{2}} \begin{pmatrix} m_\pi^2 f_\pi & 0 & 0 \\ 0 & m_\pi^2 f_\pi & 0 \\ 0 & 0 & 2m_K^2 f_K - m_\pi^2 f_\pi \end{pmatrix}. \quad (\text{A3})$$

(4) The baryon matrix, B :

$$B = \frac{1}{\sqrt{2}} b^a \lambda_a = \begin{pmatrix} \frac{\Sigma^0}{\sqrt{2}} + \frac{\Lambda^0}{\sqrt{6}} & \Sigma^+ & p \\ \Sigma^- & -\frac{\Sigma^0}{\sqrt{2}} + \frac{\Lambda^0}{\sqrt{6}} & n \\ \Xi^- & \Xi^0 & -2\frac{\Lambda^0}{\sqrt{6}} \end{pmatrix}. \quad (\text{A4})$$

-
- [1] L. Tolos and L. Fabbietti, *Prog. Part. Nucl. Phys.* **112**, 103770 (2020).
- [2] P. Papazoglou, D. Zschesche, S. Schramm, J. Schaffner-Bielich, H. Stöcker, and W. Greiner, *Phys. Rev. C* **59**, 411 (1999).
- [3] A. Hayashigaki, *Phys. Lett. B* **487**, 96 (2000).
- [4] D. B. Kaplan and A. E. Nelson, *Phys. Lett. B* **175**, 57 (1986).
- [5] E. Jenkins and A. Manohar, *Phys. Lett. B* **255**, 558 (1991); **259**, 353 (1991).
- [6] L. Tolós, J. Schaffner-Bielich, and A. Mishra, *Phys. Rev. C* **70**, 025203 (2004).
- [7] L. Tolós, J. Schaffner-Bielich, and H. Stöcker, *Phys. Lett. B* **635**, 85 (2006).
- [8] L. Tolós, A. Ramos, and T. Mizutani, *Phys. Rev. C* **77**, 015207 (2008).
- [9] A. Cieplý, E. Friedman, A. Gal, and J. Mareš, *Nucl. Phys. A* **925**, 126 (2014).
- [10] X. H. Zhong, G. X. Peng, Lei Li, and P. Z. Ning, *Phys. Rev. C* **73**, 015205 (2006).
- [11] T. Waas and W. Weise, *Nucl. Phys. A* **625**, 287 (1997).
- [12] R. Vogt, *Ultra-relativistic Heavy-Ion Collisions* (Elsevier, Amsterdam, 2007).
- [13] R. Rapp, D. Blaschke, and P. Crochet, *Prog. Part. Nucl. Phys.* **65**, 209 (2010).
- [14] Y. Nambu and G. Jona-Lasinio, *Phys. Rev.* **122**, 345 (1961).
- [15] K. Fukushima, *Phys. Lett. B* **591**, 277 (2004).
- [16] K. Kashiwa, H. Kouno, M. Matsuzaki, and M. Yahiro, *Phys. Lett. B* **662**, 26 (2008).
- [17] S. K. Ghosh, S. Raha, R. Ray, K. Saha, and S. Upadhyaya, *Phys. Rev. D* **91**, 054005 (2015).
- [18] J. Hofmann and M. F. M. Lutz, *Nucl. Phys. A* **763**, 90 (2005).
- [19] A. Mishra, K. Balazs, D. Zschesche, S. Schramm, H. Stöcker, and W. Greiner, *Phys. Rev. C* **69**, 024903 (2004).
- [20] A. Mishra and S. Schramm, *Phys. Rev. C* **74**, 064904 (2006).
- [21] A. Kumar and A. Mishra, *Phys. Rev. C* **82**, 045207 (2010).
- [22] A. Kumar and A. Mishra, *Eur. Phys. J. A* **47**, 164 (2011).
- [23] R. Kumar and A. Kumar, *Phys. Rev. C* **101**, 015202 (2020).
- [24] R. Kumar and A. Kumar, *Eur. Phys. J. C* **79**, 403 (2019).
- [25] R. Kumar and A. Kumar, *Chin. Phys. C* **43**, 12 (2019).
- [26] R. Kumar and A. Kumar, *Phys. Rev. C* **102**, 045206 (2020).
- [27] A. Mishra, E. L. Bratkovskaya, J. Schaffer-Bielich, S. Schramm, and H. Stöcker, *Phys. Rev. C* **69**, 015202 (2004).
- [28] A. Mishra, A. Kumar, S. Sanyal, and S. Schramm, *Eur. Phys. J. A* **41**, 205 (2009).
- [29] P. A. M. Guichon, *Phys. Lett. B* **200**, 235 (1988).
- [30] S. W. Hong and B. K. Jennings, *Phys. Rev. C* **64**, 038203 (2001).
- [31] K. Tsushima, D. H. Lu, A. W. Thomas, K. Saito, and R. H. Landau, *Phys. Rev. C* **59**, 2824 (1999).
- [32] A. Sibirtsev, K. Tsushima, and A. W. Thomas, *Eur. Phys. J. A* **6**, 351 (1999).
- [33] K. Saito and A. W. Thomas, *Phys. Lett. B* **327**, 9 (1994).
- [34] P. K. Panda, A. Mishra, J. M. Eisenberg, and W. Greiner, *Phys. Rev. C* **56**, 3134 (1997).
- [35] S. Chatterjee and K. A. Mohan, *Phys. Rev. D* **85**, 074018 (2012).
- [36] B. J. Schaefer, M. Wagner, and J. Wambach, *Phys. Rev. D* **81**, 074013 (2010).
- [37] L. J. Reinders, H. R. Rubinstein, and S. Yazaki, *Nucl. Phys. B* **186**, 109 (1981).
- [38] T. Hilger, R. Thomas, and B. Kämpfer, *Phys. Rev. C* **79**, 025202 (2009).
- [39] L. J. Reinders, H. R. Rubinstein, and S. Yazaki, *Phys. Rep.* **127**, 1 (1985).
- [40] F. Klingl, N. Kaiser, and W. Weise, *Nucl. Phys. A* **624**, 527 (1997).
- [41] F. Klingl, S. Kim, S. H. Lee, P. Morath, and W. Weise, *Phys. Rev. Lett.* **82**, 3396 (1999).
- [42] Q. Haider and L. C. Liu, *Phys. Lett. B* **172**, 257 (1986).
- [43] Liu and Q. Haider, *Phys. Rev. C* **34**, 1845 (1986).
- [44] H. C. Chiang, E. Oset, and L. C. Liu, *Phys. Rev. C* **44**, 738 (1991).
- [45] K. Tsushima, D. H. Lu, A. W. Thomas, and K. Saito, *Phys. Lett. B* **443**, 26 (1998).
- [46] T. Inoue and E. Oset, *Nucl. Phys. A* **710**, 354 (2002).
- [47] W. Teng-Teng, *Chin. Phys. C* **34**, 460 (2010).
- [48] C. Y. Song, X. H. Zhong, L. Li, and P. Z. Ning, *EPL* **81**, 4 (2008).

- [49] J. C. Peng *et al.*, *Phys. Rev. Lett.* **58**, 2027 (1987).
- [50] G. Martinez *et al.*, *Phys. Rev. Lett.* **83**, 1538 (1999).
- [51] G. Agakishiev *et al.*, *Phys. Rev. C* **88**, 024904 (2013).
- [52] F.-D. Berg *et al.*, *Phys. Rev. Lett.* **72**, 977 (1994).
- [53] E. Chiavassa, G. Dellacasa, N. De Marco, C. De Oliveira Martins, M. Gallio, P. Guaita, A. Musso, A. Piccotti, E. Scomparin, and E. Vercellin, *EPL* **41**, 365 (1998).
- [54] R. Averbeck, R. Holzmann, V. Metag, and R. S. Simon, *Phys. Rev. C* **67**, 024903 (2003).
- [55] D. Zschesche, A. Mishra, S. Schramm, H. Stöcker, and W. Greiner, *Phys. Rev. C* **70**, 045202 (2004).
- [56] R. Kumar, R. Chhabra, and A. Kumar, *Eur. Phys. J. A* **56**, 278 (2020).
- [57] A. Kumar, *Adv. High Energy Phys.* **2014**, 549726 (2014).
- [58] R. Chhabra and A. Kumar, *Eur. Phys. J. A* **53**, 105 (2017).
- [59] R. Chhabra and A. Kumar, *Eur. Phys. J. C* **77**, 726 (2017).
- [60] R. Chhabra and A. Kumar, *Phys. Rev. C* **98**, 025205 (2018).
- [61] G. E. Brown, C.-H. Lee, M. Rho, and V. Thorsson, *Nucl. Phys. A* **567**, 937 (1994).
- [62] C.-H. Lee, G. E. Brown, D.-P. Min, and M. Rho, *Nucl. Phys. A* **585**, 401 (1995).
- [63] N. Kaiser, P. B. Siegel, and W. Weise, *Nucl. Phys. A* **594**, 325 (1995).
- [64] S. Weinberg, *Phys. Rev.* **166**, 1568 (1968).
- [65] S. Coleman, J. Wess, and B. Zumino, *Phys. Rev.* **177**, 2239 (1969).
- [66] D. Zschesche, Description of hot, dense, and strange hadronic matter in a chiral $SU(3)_L \times SU(3)_R \sigma$ model, diploma thesis, Goethe University, Frankfurt, Germany, 1997.
- [67] W. A. Bardeen and B. W. Lee, *Phys. Rev.* **177**, 2389 (1969).
- [68] I. Zakout, H. R. Jaqaman, S. Pal, H. Stöcker, and W. Greiner, *Phys. Rev. C* **61**, 055208 (2000).
- [69] P. Wang, Z. Y. Zhang, Y. W. Yu, R. K. Su, and Q. Song, *Nucl. Phys. A* **688**, 791 (2001).
- [70] S. R. Parvathreddy, A. Jahan, N. Dhale, A. Mishra, and J. Schaffner-Bielich, *Phys. Rev. C* **97**, 065208 (2018).
- [71] P. A. Zyla (Particle Data Group) *et al.*, *Prog. Theor. Exp. Phys.* **2020**, 083C01 (2020).
- [72] L. Burakovsky and T. Goldman, [arXiv:hep-ph/9708498v1](https://arxiv.org/abs/hep-ph/9708498v1).
- [73] A. Mishra, S. Schramm, and W. Greiner, *Phys. Rev. C* **78**, 024901 (2008).
- [74] T.-S. Park, D.-P. Min, and M. Rho, *Phys. Rep.* **233**, 341 (1993).
- [75] V. E. Lyubovitskij, Th. Gutsche, A. Faessler, and E. G. Drukarev, *Phys. Rev. D* **63**, 054026 (2001).
- [76] S. J. Dong, J.-F. Lagaë, and K. F. Liu, *Phys. Rev. D* **54**, 5496 (1996).
- [77] T. Hatsuda and T. Kunihiro, *Phys. Rep.* **247**, 221 (1994).
- [78] H. Georgi, *Weak Interactions and Modern Particle Theory* (Benjamin/Cummings, Menlo Park, CA, 1984).
- [79] H. D. Politzer and M. B. Wise, *Phys. Lett. B* **273**, 156 (1991).
- [80] A. M. Green and S. Wycech, *Phys. Rev. C* **71**, 014001 (2005).
- [81] F. Renard *et al.*, *Phys. Lett. B* **528**, 215 (2002).
- [82] R. A. Arndt, W. J. Briscoe, T. W. Morrison, I. I. Strakovsky, R. L. Workman, and A. B. Gridnev, *Phys. Rev. C* **72**, 045202 (2005).
- [83] A. M. Green and S. Wycech, *Phys. Rev. C* **60**, 035208 (1999).
- [84] J. Chen, Z.-Q. Feng, P.-H. Chen, F. Niu, Y.-F. Guo, and J.-S. Wang, *Eur. Phys. J. A* **53**, 128 (2017).
- [85] J. C. David, A. Boudard, J. Cugnon, J. Hirtz, S. Leray, D. Mancusi, and J. L. Rodriguez-Sanchez, *Eur. Phys. J. Plus* **133**, 253 (2018).